Progress in Natural Science: Materials International 2013;23(1):36–43

Chinese Materials Research Society

Progress in Natural Science: Materials International

www.elsevier.com/locate/pnsmi
www.sciencedirect.com

ORIGINAL RESEARCH

Size-dependent optical properties of Au nanorods

S.L. Smitha[a,c], K.G. Gopchandran[a,*], N. Smijesh[b], Reji Philip[b]

[a]*Department of Optoelectronics, University of Kerala, Thiruvananthapuram-695 581, India*
[b]*Raman Research Institute, C.V. Raman Avenue, Sadashivanagar, Bangalore 560080, India*
[c]*St.Joseph's College for Women, Alappuzha-688 001, India*

Received 8 July 2012; accepted 10 October 2012
Available online 26 February 2013

KEYWORDS

Au nanorods;
SERS;
Crystal violet;
Z-scan;
Nonlinear absorption;
Optical limiting

Abstract In the fast evolving field of nanoscience and nanotechnology, where size and shape are crucial in deciding the optoelectronic properties of nanomaterials, the understanding of size and shape dependent behavior is of direct relevance to device applications. Present study reports the synthesis of Au nanorods with well controlled aspect ratios, and the influence of the aspect ratio on the surface enhanced Raman scattering (SERS) activity using crystal violet (CV) as the probe molecule. The influence of pH and the concentrations of reducing agent and Ag ions in controlling the aspect ratio of gold nanorods are also investigated. The structural and optical properties of the synthesized samples have been characterized by transmission electron microscopy (TEM) and UV–visible absorption spectroscopy. The nonlinear optical (NLO) transmission of the Au nanorods investigated using the open aperture Z-scan technique revealed the absorption saturation followed by an optical limiting behavior, which may find potential applications in optoelectronic nanodevices.

1. Introduction

Anisotropic metallic nanoparticles like rods have recently attracted a lot of attention due to their distinctive optical properties which lead to device applications such as nanoprobes, plasmonic waveguides and optical limiters. When excited by electromagnetic radiation nanorods give rise to longitudinal and transverse surface plasmon absorption peaks corresponding to the collective oscillation of the quasi-free electrons along the long and short axes respectively. The transverse plasmon resonance is almost insensitive to the morphology of nanorod, i.e., the spectral location of the longitudinal surface plasmon resonance (LSPR) can be easily tuned from green to NIR by modifying the nanorod aspect ratio [1]. On the basis of these properties, noble metal nanorods are considered to be good candidates for different applications such as nanoparticle mediated hyperthermal cancer therapy, optical data storage, and surface enhanced Raman scattering (SERS) [2]. Since its discovery SERS has served as a valuable tool in analytical chemistry in the

*Corresponding author.
E-mail address: gopchandran@yahoo.com (K.G. Gopchandran).
Peer review under responsibility of Chinese Materials Research Society.

ELSEVIER Production and hosting by Elsevier

1002-0071 © 2013 Chinese Materials Research Society. Production and hosting by Elsevier B.V. All rights reserved.
http://dx.doi.org/10.1016/j.pnsc.2013.01.005

characterization of compounds owing to the wealth of structural information it can provide. It is a powerful spectroscopic technique capable of non-destructive and highly sensitive characterization down to single molecule levels.

The SERS phenomenon is often described in terms of the electromagnetic as well as chemical enhancement mechanisms. By the electromagnetic mechanism, when the wavelength of incident light is close to the surface plasmon resonance, molecules adsorbed or in close proximity to the surface experience an exceptionally large electromagnetic field, resulting in Raman signal enhancement. The magnitude of electromagnetic enhancement is highly dependent on the plasmon absorption of the SERS substrate [3,4]. On the other hand chemical enhancement depends on the nature of the molecule, and results from an increased molecular polarizability by the formation of a charge transfer complex between the metal surface and the adsorbed molecule. The electronic transitions of many charge transfer complexes are in the visible region, which leads to a resonance Raman enhancement. The enhancement factors for different molecules can be different on identical SERS substrates.

In general SERS requires the use of rough surfaces of conductive materials or metal colloids, and therefore, spheroidal or rod shaped Ag and Au nanoparticles are of significant interest as SERS substrates. The fact that for rods the LSPR can be tuned is often exploited to increase the contribution of electromagnetic enhancement mechanism. The most common SERS substrates are metal particles dispersed in a colloidal suspension, rough surfaces of electrodes, and metal island films. The presence of nanostructured metal surfaces is essential for obtaining an efficient coupling between the incident radiation and the plasmon resonance bands of the substrate, whose wavelengths depend on the size and shape of the metal nanoparticles. In addition, SERS provides the possibility to acquire information specifically from the surface of materials. This trace analytical capability at the nanoscale can be used, for example, to track the migration of molecules inside cells and to design integrated cellular probes [5–8]. Single molecule detection has been reported [9] with enhancement factors as large as 10^{14}. Since the introduction of the SERS phenomenon on roughened Ag electrodes, much attention has been given to SERS on colloidal substrates of either Au or Ag to maximize the Raman signals [10–13].

Murphy and coworkers [13] have studied the aspect ratio dependence on SERS using Au and Ag nanorods and observed an enhancement in activity upon the coupling of the localized surface plasmon of Au nanorods. El-Sayed and coworkers [14] have investigated and compared the SERS property of Au nanorods and Au nanospheres under the off-surface plasmon resonance condition, and concluded that Au nanorods have a stronger activity. This is attributed to the partial excitation of the LSPR band and the contribution of the chemical effect between the strong binding of the adsorbate and the {110} facets of the Au nanorods.

In the present investigation the synthesis of Au nanorods of different aspect ratios by a seed mediated technique is reported. The influence of various parameters like the silver ion concentration, seed concentration, ascorbic acid concentration and pH of the growth solution on the aspect ratio of the Au nanorods is discussed. Au nanorods grown under optimum conditions has been then tested for Raman enhancement using crystal violet (CV) as probing molecule, and the influence of aspect ratio on the enhancement factor is investigated. The prepared nanoparticles exhibit efficient SERS properties, and their SERS activities are found to be highly dependent on the aspect ratio. Investigations of the nonlinear transmission of Au nanorods in an aqueous suspension has been carried out using open aperture Z-scan employing 7 ns laser pulses at 532 nm, and the results are discussed in detail.

2. Experimental

2.1. Materials

Hydrogen tetrachloroaurate ($HAuCl_4 \cdot 3H_2O$, 99.99%), silver nitrate ($AgNO_3$, 99.99%), sodium borohydride ($NaBH_4$, 99.99%) and crystal violet (CV, 99.9%) were purchased from Sigma Aldrich. Cetyltrimethylammonium bromide (CTAB, 99%) and ascorbic acid (98%) were obtained from Alfa Aesar. Deionized water was used throughout the experiments.

2.2. Instrumentation

UV–visible absorption spectra were recorded using Jasco V-550 UV–vis spectrophotometer with the samples in 1 cm optical path quartz cuvette. The shape and size of the particles were obtained using FEI TECNAI 30 G^2 S-TWIN transmission electron microscope. The SERS spectra were collected with a Renishaw invia microRaman spectroscopy system with a 785 nm laser as excitation source. The laser beam was focused on the samples through a 20X objective and the Raman signals were collected through the same objective in the back scattering geometry. The laser power used was 50 mW and the acquisition time was 30 s. The nonlinear transmission properties were investigated using the open aperture Z-scan method. Here the sample is moved a certain distance through the focal region of a focused laser beam, and the sample transmission is measured at small intervals of position. We used a stepper motor controlled linear translation stage to move the sample (taken in a 1 mm glass cuvette) through the beam in precise steps. The transmission of the sample at each point was measured by means of two pyroelectric energy probes (RjP7620, Laser Probe Inc.). The second harmonic output (532 nm) of a Q-switched Nd:YAG laser (Minilite, Continuum) was used for excitation. The nominal pulse width of the laser was 5 ns. The pulses were fired in the single shot mode, allowing about 1 s between successive pulses to avoid accumulative thermal effects in the sample. The experiment was automated using a program written in LabView.

2.3. Preparation of Au nanorods

Gold nanorods were prepared by a seed-mediated growth method with slight modifications [15]. Briefly, seeds are prepared by reducing 10 mL of an aqueous solution containing 0.25 mM gold tetrachloride ($HAuCl_4$) in 0.1 M cetyltrimethylammonium bromide (CTAB), adding 0.6 mL of 0.01 M sodium borohydride ($NaBH_4$). After 2 h, 10 μL of the seed solution is added to 10 mL of a growth solution consisting of 0.5 mM $HAuCl_4$ and 0.08 mM silver nitrate in 0.1 M CTAB mixed with 0.0788 M ascorbic acid. The solution was gently mixed for 1 min and then left undisturbed for 24 h to complete rod growth. The prepared Au nanorods were separated from

spheres and excess surfactants prepared by three-successive centrifugation at 14,000 rpm for 5–10 min, and re-dispersing in deionized water.

2.4. SERS sample preparation

SERS spectra of crystal violet solution were taken by adding 10 μL of 5×10^{-8} M crystal violet on 5 mL of Au nanorod solution.

3. Results and discussion

In the present study, Au nanorods are synthesized by a seed mediated approach in which CTAB stabilized spherical gold nanoparticles are used as seeds to grow into nanorod shape by a fast and successive addition of growth solutions containing gold salt, CTAB surfactant and Ag ions. Ascorbic acid is added as a weak reducing agent. In seed mediated synthesis, CTAB growth solution containing Au (III) complexes and Ag ions is added to the seeds with ascorbic acid as a chemical reductant. CTAB has been used as a surface stabilizer, which binds to the surface of nanoparticles. Surface stabilizers decrease the surface energy, control the evolution of shape and particle growth, and prevent nanoparticle coagulation. It is believed that the bromide ion forms a complex with other reactants, resulting in change in size and reactivity of the CTAB on the Au surface, thereby affecting the growth process [16].

$$[AuCl_4]^- + 4CTAB \leftrightarrow CTA{-}[AuBr_4] + 4Cl^- + 3CTA^+ \quad (1)$$

If the metallic species are involved in the formation of solute complexes or compounds, the standard redox potential will be lower since the complex is more stable than the Au ion. Thus the potential of Au complex is lower than that of Au ion. In the growth solution $[AuBr_4]^-$ exists as CTA-$[AuBr_4]^-$ which is more stable, and hence a weak reducing agent like ascorbic acid cannot reduce the complex to Au atom. Thus the nucleation can be withheld until the seed solution is added. Au nanorods have [110] surfaces along the sides and {111} on the faces. It is the growth along the {111} surfaces that leads to the elongation of Au nanorods [17,18]. Fig. 1(a) shows the variation of LSPR wavelength with reductant concentrations. From the figure it is clear that the increase in reductant concentration red-shifts the LSPR to longer wavelength region indicating an increase in aspect ratio of Au nanorods, and when the concentration of ascorbic acid is increased above 70 μL, LSPR blue-shifts.

The reduction process of Au ion by ascorbic acid can be described as [16],

$$\text{First reduction reduction} \quad Au^{3+} \rightarrow Au^{1+} \quad (2)$$

$$CTA\text{-}AuBr_4 + C_6H_8O_6 \rightarrow CTA\text{-}AuBr_2 + C_6H_6O_6 + 2H^+ + 2Br^- \quad (3)$$

Second reduction,

$$Au^{1+} \rightarrow Au^0 \quad (4)$$

$$2CTA\text{-}AuBr_2 + C_6H_8O_6 \rightarrow 2Au + C_6H_6O_6 + 2CTA^+ + 2H^+ + 4Br^- \quad (5)$$

The first reduction is confined in the metallomicelles. The second reduction begins only after the addition of seed solution.

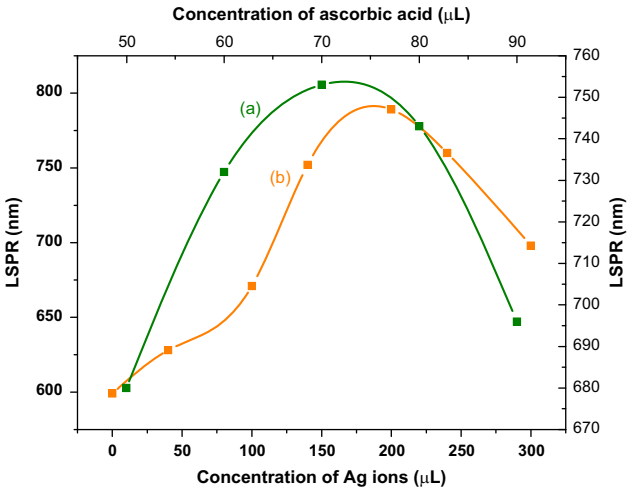

Fig. 1 Variation of LSPR wavelength with concentration of: (a) ascorbic acid and (b) Ag ions.

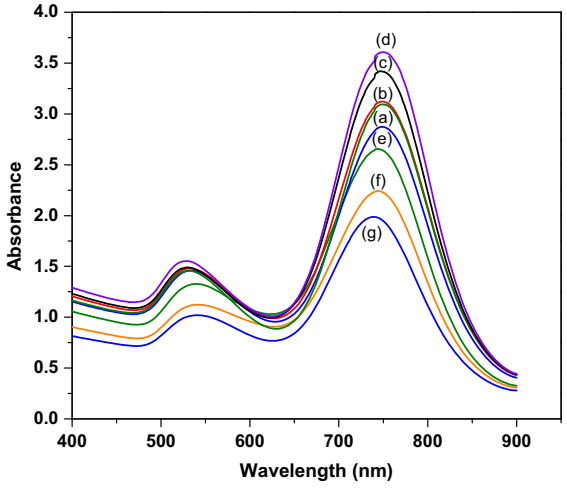

Fig. 2 UV–vis absorption spectra of Au nanorods prepared with different seed concentrations: (a) 4, (b) 6, (c) 8, (d) 10, (e) 12, (f) 15 and (g) 20 μL.

The overall reduction is

$$2CTA\text{-}AuBr_4 + 3C_6H_8O_6 \rightarrow 2Au + C_6H_6O_6 + 2CTA^+ + 6H^+ + 8Br^- \quad (6)$$

The concentration of the seed solution also plays an important role in the aspect ratio of the Au nanorods. Fig. 2 shows the UV–vis absorption spectra of Au nanorods with different seed concentrations (by fixing the concentration of other chemicals) from which it is evident that a smaller seed concentration gives rise to larger aspect ratio rods. With increase in seed concentration, the aspect ratio decreases. Studies on the variation of LSPR peak with Ag ions represented in Fig. 1(b) show that the LSPR is red-shifted with concentration of $AgNO_3$ upto 200 μL. Beyond that, a blue shift in LSPR is observed. It is proposed that the Ag^+ ion (pairing with Br^- from CTAB) binds on the [111] surfaces of growing Au nanoparticles and catalyze growth in those

directions. When Ag^+ increases, longer particles are formed as a result of more catalyzed growth [19,20]. Consequently, increasing Ag^+ leads to changing the size of nanorods and increase their aspect ratio. The negative effect of Ag ions at higher concentration is probably due to their interaction with the bromide counter ion of the surfactant monomer [20]. Fast Ag deposition followed by strong CTAB binding (via bromide) inhibits Au growth on the sides of the rods and leads to preferential growth of Au at the ends. Thus changing the Ag concentration changes the resulting nanorod dimensions and aspect ratio. Ascorbic acid is too weak to reduce Au^{3+} to Au^0. Upon the addition of ascorbic acid Au^{3+} reduces to Au^+. Reduction of Au^+ to Au^0 occurs when seed solution is added. When seed particles are introduced in a solution containing Au^+ ions, they act as nucleation centers catalyzing the reduction of Au^+ to Au^0 on their surfaces [17,21]. Fig. 3 shows the TEM image of Au nanorods synthesized with 200 and 240 μL Ag ion concentration and the aspect ratio of the nanorods formed are found to be 5.8 and 16 respectively. From the HRTEM image, the fringe spacing is measured to be 0.231 nm, which corresponds closely with the spacing between the (111) plane of fcc gold (0.235 nm) (JCPDS card no: 04-0784). The selected area electron diffraction (SAED) pattern reveals that the particles are crystalline in nature. The spots are indexed to (111), (200), (220), (311) and (222) reflections of fcc gold.

In order to study the influence of pH on the formation of nanorods, Au nanorods are prepared at different pH. The pH value of the solution is an important factor in the formation and control of morphology of the nanorods. The UV–vis absorption spectra of Au nanorods with acidic and basic pH are shown in Figs. 4 and 5. From the figure, it is evident that when the pH is lowered, the longitudinal SPR blue-shifts and under basic condition the LSPR red-shifts to higher wavelength. It is believed that the variation of the aspect ratio as a function of pH is possibly based on the destabilization of the CTAB bilayer during the growth of Au nanorods [22]. The TEM image of Au nanorods with a pH of 3 and 8 is shown in Fig. 6(a) and (b) respectively. For basic pH, the nanorods are assembled into well-ordered structures. Self-assembly of Au nanorods into ordered structures, aligning side by side, was achieved for a pH of 8 by addition of NaOH.

3.1. *SERS studies*

A solution of crystal violet was used as the probe molecule to test the quality of SERS substrate. SERS experiments were done in aqueous solutions in order to study the effect of nanorod plasmon resonance by controlling the nanorod aspect ratio. It is important that in aqueous solution nanorods are randomly oriented and their SERS spectra are representative of all possible orientations averaged over the entire acquisition

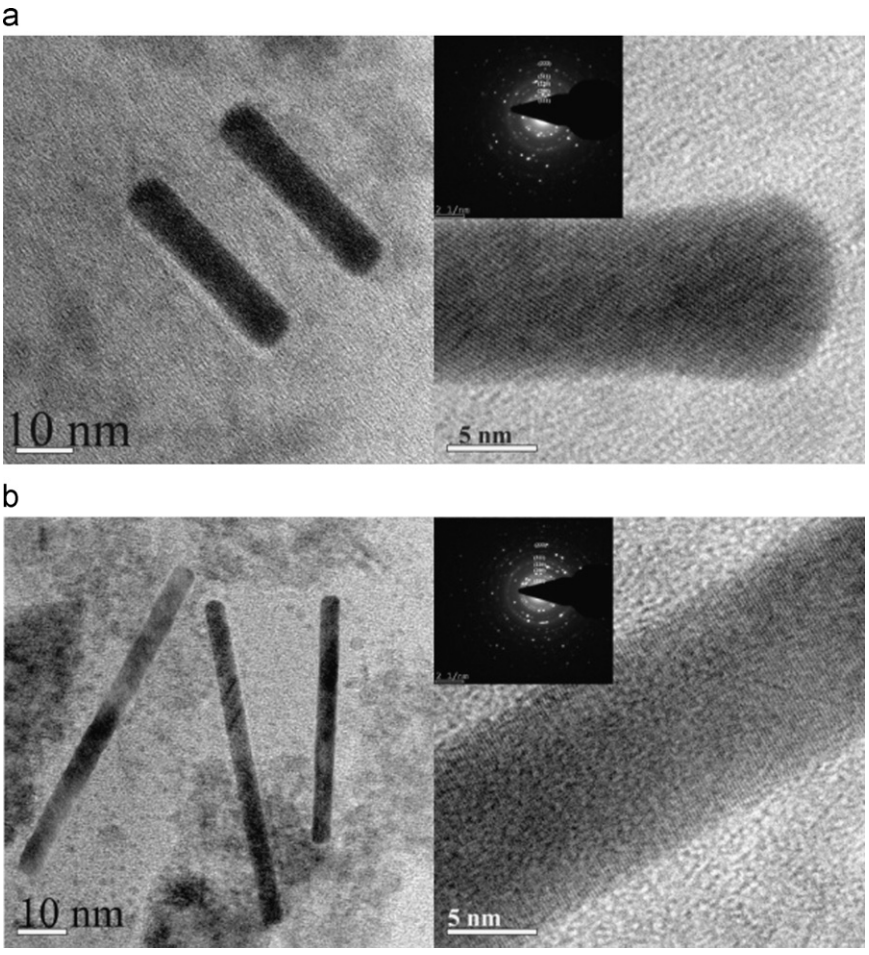

Fig. 3 TEM and HRTEM images of Au nanorods synthesized with different $AgNO_3$ concentrations: (a) 200 and (b) 240 μL. Inset shows the corresponding SAED pattern.

time. The ideal geometry would be to fix the nanorod orientation with the long axis parallel to the excitation source polarization, in order to have maximum longitudinal plasmon overlap. The normal Raman spectrum and the SERS spectrum of CV using 785 nm excitation line for Au nanorods of aspect ratio 2.4, 5.8 and 16 are given in Fig. 7. Three different groups of modes were observable for CV: modes associated with the central carbon atom (C^+-phenyl vibrations upto 450 cm^{-1}), nitrogen atoms (N-phenyl stretching, between 1350 and 1400 cm^{-1}), and phenyl rings (skeletal ring vibrations and ring C–H deformations between 400 and 1300 cm^{-1} and ring stretching modes above 1400 cm^{-1}) [21–24]. In the spectra, the C^+-phenyl bending mode was observed at 336 cm^{-1}. C–H out of plane bendings has been observed at about 726, 770 and 792 cm^{-1}, whereas ring skeletal vibrations appear at about 914, 938 and 981 cm^{-1}. The band at 1170 cm^{-1} is attributed to C–H in plane bending vibrations. N-phenyl stretching is observed at 1371 cm^{-1} and ring C–C stretching at 1538, 1582 and 1618 cm^{-1}. The strong enhancements observed for all groups of modes mentioned suggest the central carbon atom, nitrogen atoms and π electrons in the phenyl ring as possible interaction sites. The CV molecules are normally bonded to the Au surface by coulombic and Van der Waals interactions [23–27]. This is evident by the absence of Au–N stretching vibrational peak in the 225–231 cm^{-1} region of the SERS spectra. Even though all these nanorods are capped with CTAB, no characteristic vibrational modes for CTAB are observed in these spectra [28].

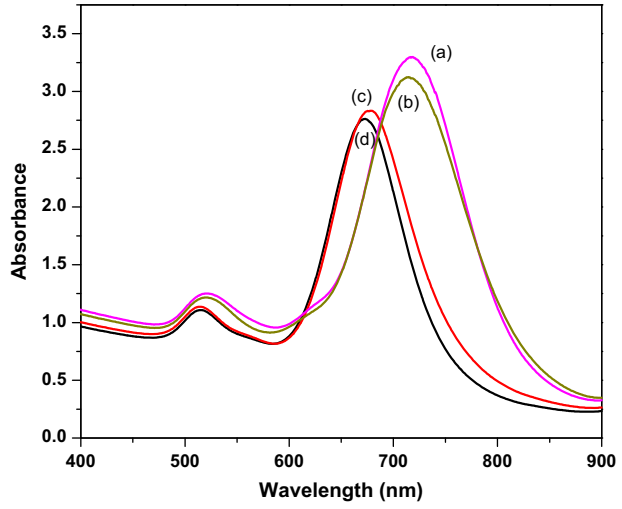

Fig. 4 UV–vis absorption spectra of Au nanorods prepared at different pH conditions: (a) 4, (b) 3, (c) 2 and (d) 1.

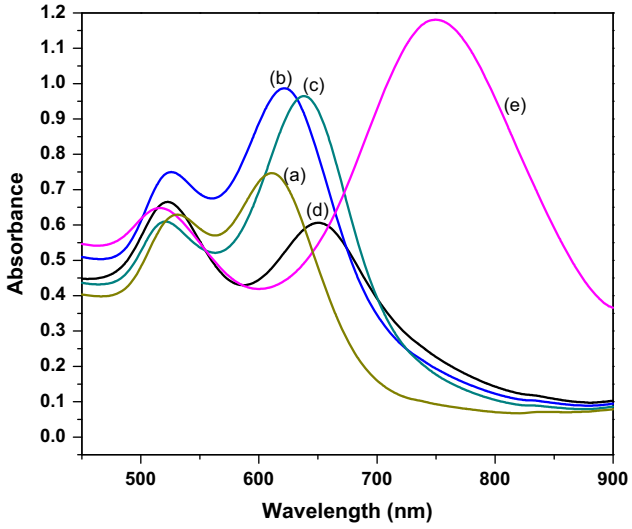

Fig. 5 UV–vis absorption spectra of Au nanorods prepared at different pH conditions: (a) 5, (b) 6, (c) 7, (d) 8 and (e) 10.

The enhancement factor (EF) is calculated using the equation [29],

$$\text{Enanaement factor(EF)} = (I_{SERS}/C_{SERS})/(I_{Normal}/C_{Bulk}) \quad (7)$$

where I_{SERS} and I_{Normal} are the intensity of the SERS and normal Raman spectra of the crystal violet solution, respectively. C_{SERS} and C_{Bulk} are the concentration of crystal violet in the SERS sample (5.8×10^{-8} M) and in the bulk sample (0.1 M), respectively.

The signal intensities of the ring C–C stretching mode at 1618 cm^{-1} in the SERS and bulk Raman spectra of the molecule were used to calculate the enhancement factor of Au nanorods of different aspect ratios. The enhancement factor is calculated using Eq. (7) and the variation of enhancement factor with aspect ratio of Au nanorods is presented in Fig. 8. Raman peaks and the corresponding assignments in the conventional and SERS spectra of CV is given in Table 1. The synthesized nanorods exhibited efficient SERS properties and their SERS activity is found to highly sensitive to the aspect ratio of the nanorods, which may be due to the electromagnetic enhancement mechanism [24]. These unique and tunable optical properties of

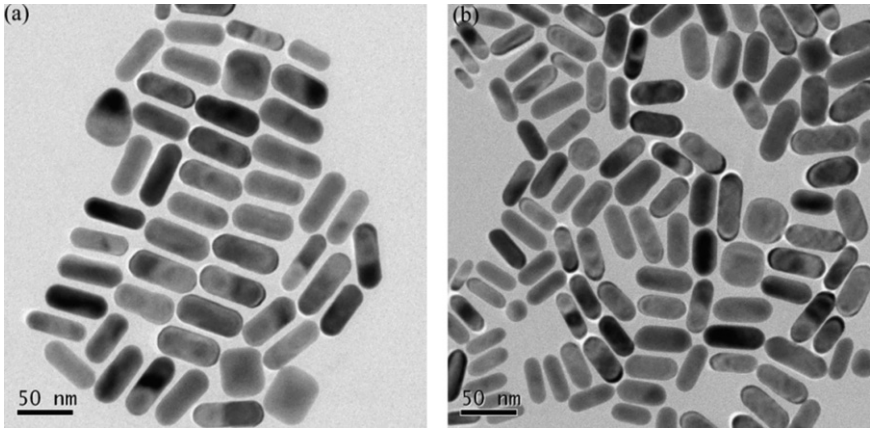

Fig. 6 TEM images of Au nanorods at different pH: (a) 3 and (b) 8.

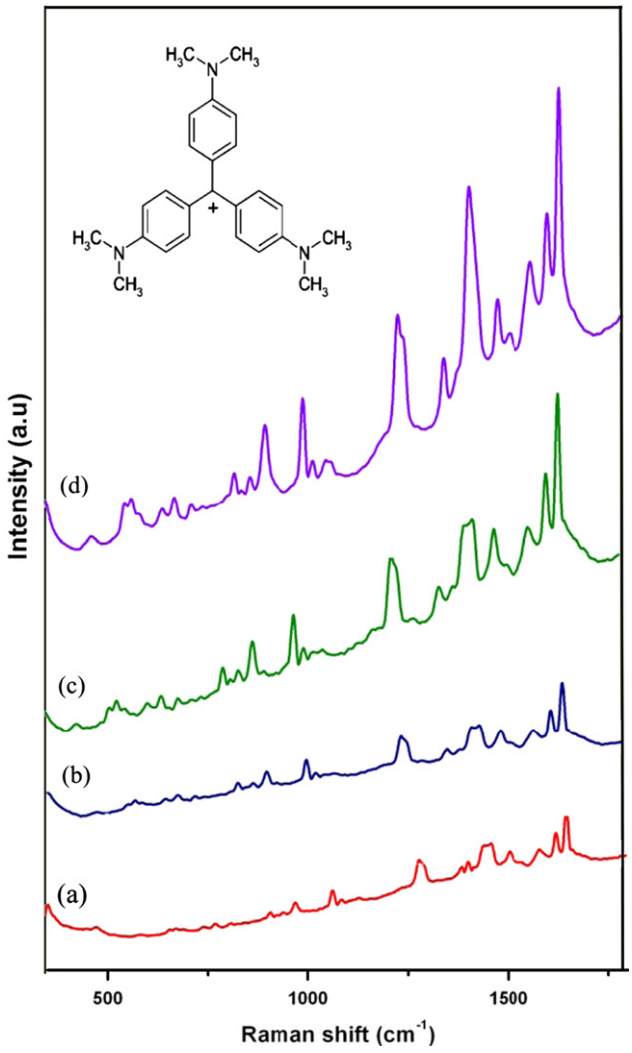

Fig. 7 (a) Normal Raman spectrum and SERS spectrum of crystal violet on Au nanorods of different aspect ratios: (b) 2.4, (c) 5.8 and (d) 16.

Au nanorods make them potential candidates for the development of sensitive chemical and biological sensors.

3.2. *Nonlinear transmission studies*

Optical limiting is an application derived from nonlinear optical transmission of a given sample, useful for the protection of human eyes and sensitive optical detectors from accidental exposure to intense light beams. The Z-scan technique can be employed for measuring nonlinear transmission. In a typical open aperture Z-scan, the transmission of the sample normalized to its linear transmission (''normalized transmittance'') is plotted against the sample position measured relative to the beam focus. Optical limiting is indicated by a valley shaped curve, symmetric about the focal ($z=0$) position. A number of reports on the optical limiting property of noble metal nanoparticles can be found in literature [30–32].

We measured the variation of the optical limiting behavior in the present gold nanorods as a function of the aspect ratio. The results are shown in Fig. 9a–d. The humps flanking the valley in the Z-scans of Fig. 9a–c indicate an absorption

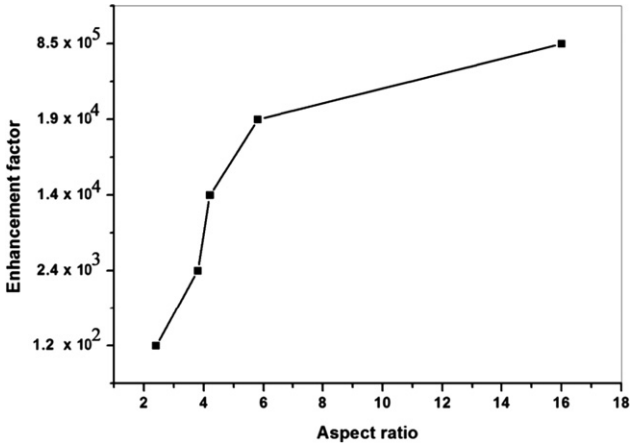

Fig. 8 Variation of SERS enhancement factor of crystal violet with aspect ratio of Au nanorods. Excitation is at 785 nm.

saturation at relatively lower input light intensities, which is related to the plasmon excitation [33]. Thus there are two causes for the nonlinearity: one is a saturation of the ground state absorption, and the other is an excited state absorption (ESA) resulting from inter-band and intra-band transitions prevalent in metallic systems. In such cases an effective nonlinear absorption coefficient $\alpha(I)$, given by

$$\alpha(I) = \frac{\alpha_0}{1 + (I/I_s)} + \beta I \tag{8}$$

can be considered, where α_0 is the unsaturated linear absorption coefficient at the wavelength of excitation, I is the input laser intensity, and I_s the saturation intensity (intensity at which the linear absorption drops to half its original value). $\beta I = \sigma N$ is the excited state absorption (ESA) coefficient, where σ is the ESA cross section and $N(I)$ is the intensity-dependent excited state population density. For calculating the transmitted intensity for a given input intensity, the propagation equation,

$$\frac{dI}{dz'} = -\left[\left(\alpha_0 / \left(1 + \frac{I}{I_s}\right)\right) + \beta I\right] I \tag{9}$$

is numerically solved. Here z' indicates the propagation distance within the sample. By determining the best-fit curves for the experimental data, the nonlinear absorption coefficient β for the nanorods of aspect ratios 2.4, 3.8, 4.2 and 5.8 are measured to be 8.5×10^{-11}, 7.8×10^{-11}, 5.7×10^{-11} and 2.3×10^{-12} m/W respectively. Thus the β value is found to decrease with increase in aspect ratio. Fig. 10 represents the variation in β with TSPR intensity and aspect ratio of Au nanorods. In comparison, when measured previously in the same experimental setup under similar conditions, the β value for Bi nanorods was around 10^{-11} m/W [34], Cu nanocomposite glasses was between 10^{-12} to 10^{-10} m/W [35], and Au–Ag core-shell nanoparticles was between 10^{-10} to 10^{-9} m/W [36].

4. Conclusions

Au nanorods have been synthesized employing the seed mediated growth approach, and the influence of parameters, such as the pH, reducing agent concentration and the Ag ions concentration in the precise control of aspect ratio of gold

Table 1 Raman peaks and the corresponding assignments in the conventional and SERS spectra of CV using an excitation of 785 nm.

Normal Raman (cm^{-1})	SERS (cm^{-1})			Assignment
	Aspect ratios			
	2.4±0.9	5.8±0.11	16±0.08	
726	726	726	726	C–H out of plane bending
770	770	770	770	C–H out of plane bending
792	792	792	792	C–H out of plane bending
914	914	914	914	Ring skeletal vibrations
938	938	938	938	Ring skeletal vibrations
981	981	981	981	Ring skeletal vibrations
1170	1178	1178	1178	C–H in plane bending
1371	1370	1370	1370	N-phenyl stretching
1534	1534	1534	1534	C–C stretching
1585	1585	1585	1585	C–C stretching
1619	1619	1619	1619	C–C stretching

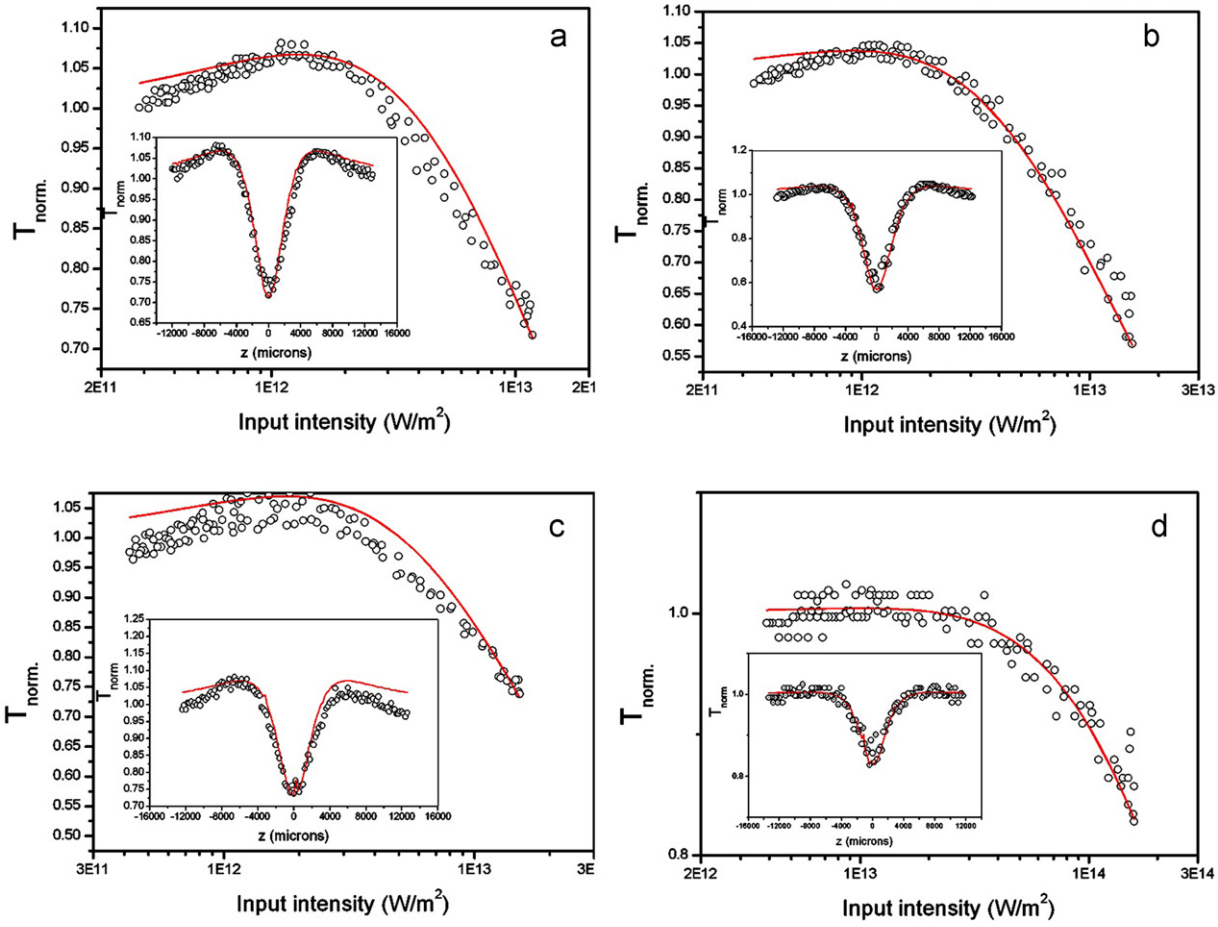

Fig. 9 Input laser intensity vs. normalized transmittance curve of gold nanorods of aspect ratio (a) 2.4, (b) 3.8, (c) 4.2, and (d) 5.8. Inset shows the corresponding open-aperture Z-scan curves. Open circles show the experimental data and the solid lines show the numerical fits obtained using Eqs. (8) and (9).

nanorods is studied. SERS studies using crystal violet as the probe molecule reveal a large Raman enhancement. The SERS activity and the enhancement factor are observed to be highly dependent on the aspect ratio of the Au nanorods. The nanorods also exhibit an efficient optical limiting behavior. These studies show that Au nanorods of controllable aspect ratio are suitable candidates for potential applications in sensing and photonics applications.

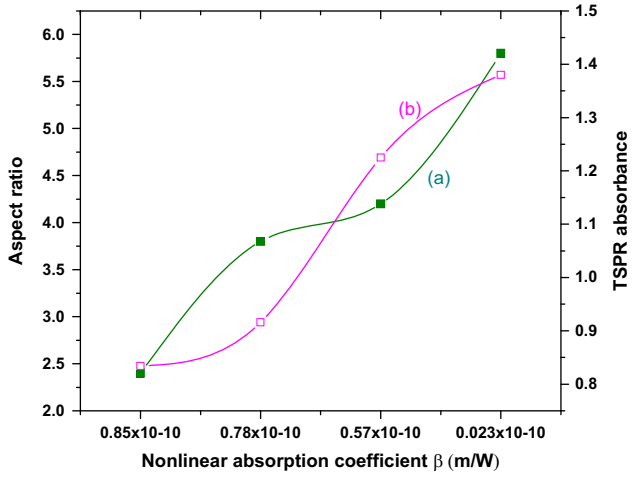

Fig. 10 Variation of nonlinear absorption coefficient (β) with (a) aspect ratio of Au nanorods and (b) TSPR intensity.

Acknowledgment

Dr. K.G. Gopchandran acknowledges University Grants Commission, New Delhi for providing financial assistance by granting major research project.

References

[1] E.N. Esenturk, A.R.H. Walker, Journal of Raman Spectroscopy 40 (2009) 86.
[2] X. Huang, S. Neretina, M.A. El-Sayed, Advanced Materials 21 (2009) 4880.
[3] C. Noguez, Journal of Physical Chemistry C 111 (2007) 3806.
[4] R. Sanci, M. Volkan, Sensors and Actuators B 139 (2009) 150.
[5] Eric Le Ru, Pable Etchegoin, in: Principles of Surface Enhanced Raman Spectroscopy and Related Plasmonic Effects, Elsevier, Amsterdam, The Netherlands, 2009.
[6] Y. Ding, Z.L. Yang, S.B. Li, X.S. Zhou, F.R. Fan, W. Zhang, Z.Y. Zhou, D.Y. Wu, B. Ren, Z.L. Wang, Z.Q. Tian, Nature 468 (2010) 392.
[7] M. Muniz-Miranda, M. Innocenti, Applied Surface Science 226 (2004) 125.
[8] A. Sabur, M. Havel, Y. Gogotsi, Journal of Raman Spectroscopy 39 (2008) 61.
[9] S. Nie, Science 275 (1997) 1102.
[10] S.S. Shandkar, A. Rai, A. Ahmad, M. Sastry, Chemistry of Materials 17 (2005) 566.
[11] R. Gebner, P. Rosch, R. Petry, M. Schimitt, M.A. Strehle, W. Kiefer, J. Popp, Analyst 129 (2004) 1193.
[12] S. Guo, Y. Wang, E. Wang, Nanotechnology 18 (2007) 405602.
[13] C.J. Orendorff, L. Gearheart, N.R. Jana, C.J. Murphy, Physical Chemistry Chemical Physics 8 (2006) 165.
[14] B. Nikoobakht, J. Wang, M.A. El-Sayed, Chemical Physics Letters 366 (2002) 17.
[15] N.R. Jana, L. Gearheart, C.J. Murphy, Journal of Physical Chemistry B 105 (2001) 4065.
[16] M.A. El-Sayed, B. Nikkobakht, Chemistry of Materials 15 (2003) 1957.
[17] W. Abidi, P.R. Selvakannan, Y. Guillet, I. Lampre, P. Beaunier, B. Pansu, B. Palpant, H. Remita, Journal of Physical Chemistry C 114 (2010) 14794.
[18] C. Yu, L. Varghese, J. Irudayaraj, Langmuir 23 (2007) 9114.
[19] M. Liu, G. Sionnest, Journal of Physical Chemistry B 109 (2004) 22192.
[20] V. Sharma, K. Park, M. Srinivasarao, Materials Science and Engineering 65 (2009) 1.
[21] C.J. Orendorff, C.J. Murphy, Journal of Physical Chemistry B 110 (2006) 3990.
[22] W.M. Park, Y.S. Huh, W.H. Hong, Current Applied Physics 9 (2009) e140.
[23] I. Persaud, W.E.L. Grossman, Journal of Raman Spectroscopy 24 (1993) 107.
[24] D. Cialla, H. Uwe, H. Schneidewind, R. Moller, J. Popp, ChemPhysChem 9 (2008) 758.
[25] J.D. Liang, E. Burstein, H. Kobayashi, Physics Review Letters 57 (1986) 1793.
[26] Y. Wang, M. Becker, L. Wang, J. Liu, R. Scholz, J. Peng, U. Gosele, S. Christiansn, D.H. Kim, M. Steinhart, Nanoletters 9 (2009) 2384.
[27] M.K. Hossain, K. Shibamoto, K. Ishiko, M. Kiajima, T. Mitani, S. Nakashima, Journal of Luminescence 122 (2007) 792.
[28] X. Huang, I.H. El-Sayed, W. Qian, M.A. El-Sayed, Nanoletters 7 (2007) 1591.
[29] Y. Wang, H. Chen, S. Dong, E. Wang, Journal of Chemical Physics 124 (2006) 074709.
[30] H.L. Elim, J. Yang, J.Y. Lee, Applied Physics Letters 88 (2006) 083107.
[31] S. Qu, Y. Song, H. Liu, Y. Wang, Y. Gao, S. Liu, X. Zhang, Y. Li, D. Zhu, Optics Communications 203 (2002) 283.
[32] J.M. Lamarre, F. Billard, C.H. Kerbou, M. Lequime, S. Roorda, L. Martinu, Optics Communications 281 (2008) 331.
[33] R. Philip, G.Ravindra Kumar, N. Sandhyarani, T. Pradeep, Physical Review B 62 (2000) 13160.
[34] S. Sivaramakrishnan, V.S. Muthukumar, S.S. Sai, K. Venkataramanaiah, J. Reppert, A.M. Rao, M. Anija, R. Philip, N. Kuthirummal, Applied Physics Letters 91 (2007) 093104.
[35] B. Karthikeyan, M. Anija, C.S. Suchand sandeep, T.M Muhammad Nadeer, R. Philip, Optics Communications 281 (2008) 2933.
[36] A.S. Nair, V. Suryanarayanan, T. Pradeep, J. Thomas, M. Anija, R. Philip, Materials Science and Engineering B 117 (2005) 173.